# Ferroelectric ordering and electroclinic effect in chiral smectic liquid crystals

Yu. G. Fokin,* T. V. Murzina, and O. A. Aktsipetrov
*Physics Department, Moscow State University, Moscow 119992, Russia*

S. Soria† and G. Marowsky
*Laser-Laboratorium Goettingen e.V., Hans-Adolf-Krebs-Weg 1, D-37077 Goettingen, Germany*
(Received 30 May 2003; published 4 March 2004)

Ferroelectric ordering, the electroclinic effect, and chiral smectic $C(\mathrm{Sm}C^*)$–smectic $A$ phase transitions in thin planar ferroelectric liquid crystal (FLC) cells are studied by means of linear electro-optic and second harmonic generation (SHG) techniques. The ferroelectric switching is detected in biased FLC cells by measuring azimuthal dependences of linear and nonlinear responses. The applied dc electric field rotates the FLC symmetry axis with initial and final orientations in the cell plane. Comparative studies of the SHG switching behavior in reflection and transmission geometries allows one to distinguish the contributions from the bulk and the subsurface layers of the cell. The analysis of SHG temperature dependences shows the existence of a strong surface coupling. The temperature-dependent nonlinear polarization shows a critical behavior with the exponent $\sim 0.3$ in Sm$C^*$ phase.

DOI: 10.1103/PhysRevE.69.031701 PACS number(s): 64.70.Md, 42.65.Ky, 77.80.Fm, 61.30.Hn

## I. INTRODUCTION

Ferroelectric liquid crystals (FLC) have been studied intensively for several decades. Chiral smectic liquid crystals (LC) have unique material properties such as spontaneous polarization [1]. Although a single chiral smectic LC molecule has a nonzero dipole moment due to symmetry considerations [2], LC molecules in the bulk of the sample tend to form a helical structure which leads to polarization compensation. The helix can be unwound by application of a strong electric field or using thin test cells. Conventionally, the alignment of LC molecules is obtained by unidirectional mechanical rubbing of a thin polymer layer which coats the inner cell surfaces. Thus, the LC molecules point their long axes along the rubbing direction. This anisotropic interaction influences the ferroelectric ordering and the switching behavior which are of great practical importance for any LC device. The ferroelectrically ordered smectic $C$ (Sm$C^*$) phase is characterized by a nonzero angle between the molecular long axis and the smectic layer normal. This tilt angle is the order parameter which is used to describe the second-order Sm$C^*$–Sm$A^*$ (smectic $A$) phase transition.

In several studies the temperature dependence of the tilt angle below the critical temperature follows a power law of 0.5 (classical behavior) [3], whereas in other studies it follows a power law of 0.3, in strong analogy with the superfluid helium predicted by de Gennes [4]. The Sm$A^*$ phase in the vicinity of the transition point has also been the subject of intensive investigations, since in that part of the critical region the electroclinic (EC) effect can induce a tilt angle which is proportional to the electric-field strength [5]. The induced tilt angle is also strongly temperature dependent and increases while approaching the phase transition temperature. Another type of this phenomenon, the so-called surface EC effect, is observed in the interfacial region of the FLC cells and originates from the interaction of the subsurface layers of chiral smectic LC molecules and a localized surface field [6]. In the vicinity of the transition point, the critical exponents of the tilt angle are in the range of 0.5–1.5 [4–7]. The surface EC effect results in the existence of subsurface region in which the director is twisted from the rubbing axis to the bulk alignment direction. The ferroelectric properties of this region are of great importance as they play the dominant role in LC devices.

In this paper we use linear electro-optic (EO) and second harmonic generation (SHG) techniques for investigation of ferroelectric ordering, Sm$C^*$–Sm$A^*$ phase transitions, and the EC effect in thin FLC cells. The main emphasis is made on comparative studies of the SHG reflection and transmission experimental geometries in order to figure out the role of subsurface layers and the bulk in ferroelectric phase transitions. The SHG method is well known for its sensitivity to symmetrical, structural, and electronic properties of surfaces, interfaces, and ultrathin films, and has been widely used along with EO for studying ferroelectric properties of chiral smectic LC [8]. As the SHG response strongly depends on the polar state of the matter because of its unique sensitivity to the breakdown of the inversion symmetry [9], it is a powerful instrument for probing ferroelectric phase transitions and electric-field-induced effects in the vicinity of the critical region.

## II. MODEL DESCRIPTION

We studied linear and nonlinear quadratic responses of the FLC cells upon application of an electric field and temperature variation up to the Sm$C^*$–Sm$A^*$ phase transition. Chiral smectic LC belong to the $C_2$ point group symmetry with the symmetry axis oriented in the cell plane. A schematic representation of the FLC cell and the coordinate system is

*Electronic address: yura@shg.ru; URL: http://www.shg.ru
†Present address: ICFO–Institut de Ciencies Fotoniques and Dept. of Signal Theory and Communications, Universitat Politecnica de Catalunya, 08034 Barcelona, Spain.

 

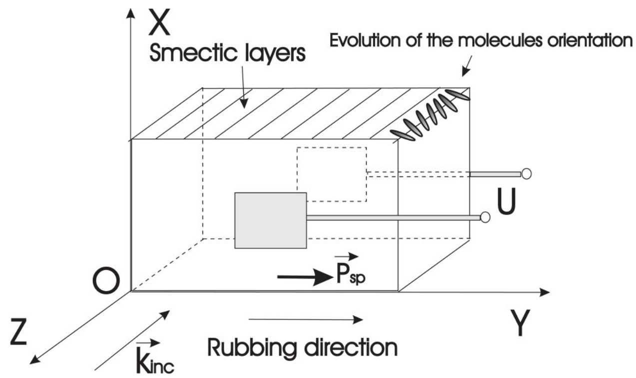


FIG. 1. Schematic representation of experimental geometry.

shown in Fig. 1. In this coordinate frame $OZ$ is the normal to the cell, $XY$ is the cell plane, and the $C_2$ axis is parallel to the $OY$ direction and coincides with the main optical axis. We assume the FLC cell to be uniaxial, with the ordinary and extraordinary refractive indices $n_0 = n_x = n_z$ and $n_e = n_y$, respectively. The transmittance of an optically active plate of thickness $d$ and birefringence $\Delta n$ at the wavelength $\lambda$ in crossed-polarizers geometry is determined by the equation

$$T = \sin^2(2\alpha)\sin^2\frac{\Delta n \pi d}{\lambda}, \tag{1}$$

where $\alpha$ is the angle between the main optical axes and the polarization direction of the incident light. The linear electro-optic tensor $r_{ijk}$, where indices $i$, $j$, $k$ denote the axes of the cell coordinate system, has eight nonvanishing components $r_{xxy}$, $r_{yyy}$, $r_{zzy}$, $r_{yzx}$, $r_{yzz}$, $r_{xzy}$, $r_{xyx}$, $r_{xyz}$ [10]. Application of the dc electric field $E$ along $OZ$ direction leads to the rotation of the optical axes, which could be interpreted in terms of the rotation of the ellipse of refractive indices. The equation of index ellipsoid in the presence of the electric field $E$ has the form

$$\frac{x^2}{n_x^2} + \frac{y^2}{n_y^2} + \frac{z^2}{n_z^2} + 2yzr_{yzz}E + 2xyr_{xyz}E = 1. \tag{2}$$

The transformation of Eq. (2) to the canonical form gives the dc field-induced rotation of the undisturbed system of coordinates based on the main optical axes. Considering the rotation only around $OZ$ axis, the influence of the electric field can be described by the tilt of the main optical axis in the cell plane with the dependence of the turn angle $\Delta\alpha$ on the electric field as

$$\Delta\alpha = \frac{1}{2}\arctan\frac{2r_{xyz}E}{\frac{1}{n_o^2} + \frac{1}{n_e^2}}. \tag{3}$$

The nonlinear quadratic susceptibility tensor of the FLC cell with $C_2$ symmetry is given by following nonvanishing components $\chi_{ijk}$, $\chi_{yxx}$, $\chi_{yyy}$, $\chi_{yzz}$, $\chi_{yzx}$, $\chi_{xyz}$, $\chi_{xxy}$, $\chi_{zyz}$, $\chi_{zxy}$ [11]. The contribution of each quadratic susceptibility component to the SHG intensity depends on the angle of incidence of the fundamental radiation, on the azimuthal position of the sample, and on polarizations of the input and SHG light. In transmission geometry at normal incidence only three components of quadratic susceptibility participate in SHG, $\chi_{yxx}$, $\chi_{xxy}$, and $\chi_{yyy}$, and for *pp* geometry the SHG intensity can be expressed by

$$I_{pp}^{2\omega} \sim \cos^2\theta[\chi_{yyy}\cos^2\theta + (2\chi_{xxy} + \chi_{yxx})\sin^2\theta]^2, \tag{4}$$

where the azimuthal angle $\theta$ is the angle between the direction of the $p$ polarization and $C_2$ axis of the cell symmetry. By fitting the anisotropy dependences of the SHG intensity in all combinations of polarizations, the corresponding components of the quadratic susceptibility can be extracted.

According to a well-known model, in the smectic planar layers FLC molecules can precess on the surface of the smectic cone [12]. Ferroelectric switching is attributed to the interaction between the molecular dipoles and external electric field and results in rotation of the molecules and, correspondingly, of the symmetry axes within half of the smectic cone. If the molecular director positions, corresponding to the saturating electric fields of the opposite values, are in the cell plane and on the opposite sides of the smectic cone, then Eq. (3) can be used for the explanation of ferroelectric switching probed by optical methods, as it shows the in-plane rotation of the main optical axis.

The angle between the molecular long axis and the normal to the smectic layers, i.e., the apex angle of the cone, is the order parameter of the Sm$C$*–Sm$A$* phase transition, vanishing in the Sm$A$* phase. It can also have a finite magnitude in the Sm$A$* phase in the vicinity of the critical temperature due to the EC effect. The temperature-induced changes of this angle lead to the changes in $\alpha$ and $\theta$ angles which are determined by the orientation of the main axis. We show below that the temperature and electric-field dependences of the main axis orientation can be deduced from linear and nonlinear-optical experiments, in order to describe the ferroelectric switching, phase transitions, and the EC effect in FLC cells.

## III. EXPERIMENT

The principal arrangement of the experimental setup is described elsewhere [13]. Briefly, an optical parametric oscillator (OPO) laser system is used as a source of the fundamental radiation, with the output wavelength of 537 nm, repetition rate 10 Hz, and pulse duration 4 ns. An appropriate set of color filters is used for linear- and nonlinear-optical measurements. A photodiode or a photomultiplier tube and gated electronics are used as a registration system for linear or nonlinear experiments. The temperature is varied from 20 to 55 °C and automatically controlled by a digital thermocouple thermometer with the accuracy of about 1 °C. An electric field in the range of −15 to +15 MV/m is applied along $OZ$ axis through the indium tin-oxide (ITO) electrodes. Commercial FLC cells (E.H.C. Co., Tokyo) of a nominal thickness of 2 $\mu$m are used. These cells contain glass plates, ITO electrodes, and unidirectional rubbed polyamide surface layers. The samples are prepared by a slow cooling of the mixture

[13], capillary filled in the isotropic phase. The critical temperature of the Sm$C^*$-Sm$A^*$ phase transition for the studied mixture is about 42 °C. The SHG and linear-optical transmittance of the empty cell are studied in the temperature region of Sm$C^*$ and Sm$A^*$ phases to determine its nonlinear quadratic susceptibility and optical activity which can decrease the contrast of the measured effects in FLC cells. Anisotropy dependences of linear and nonlinear responses from the regions of the empty cell with and without ITO layers are studied. The dependences reveal fully isotropic character for *p*-polarized SHG due to the in-plane symmetric structure of the ITO electrodes and glass walls of the cells. The intensity of the *p*-polarized SHG from the empty cell both in reflection geometry and in transmission at normal incidence of the fundamental beam is comparable with the SHG intensity in the minimum of the anisotropic SHG dependences.

To prove the regular character of the nonlinear response from FLC cells, the SHG spectrum, indicatrix, and the SHG intensity dependence on the incident laser power are studied. The spectrum is studied using a monochromator placed prior to the registration system, and revealed a maximum in the region of the double frequency of the fundamental radiation. Along with the quadratic dependence of the SHG intensity vs input power of the incident light it indicates that nonlinear-optical response from the FLC cells is of the second order. The angular dependence of the scattered SHG has a sharp maximum in the direction of the specular reflection, similar to that observed previously for similar samples [13]. The ratio of the specular and diffuse SHG intensities is about $10^3$, which indicates a dominantly regular character of the nonlinear quadratic response from the FLC cells.

To determine the in-plane components of the nonlinear susceptibility, the SHG intensity dependence vs azimuthal angle is measured at normal incidence in transmission geometry for different polarization combinations *pp*, *ss*, *ps*, *sp*, where the first letter denotes the polarization of the incident light and the second one denotes polarization of the light transmitted through the analyzer placed after the sample. The observed anisotropy is shown in Figs. 2(a) and 2(b) and correlates well with the dependence (4), obtained for a $C_2$ symmetry structure. These dependences are measured in the absence of the dc electric field.

Ferroelectric switching of the cells is studied by measuring the anisotropy dependences of the SHG intensity at different values of the external dc electric field applied along the normal to the cell plane. Figure 3(a) shows the SHG intensity measured in the transmission geometry for *pp* combination of polarizations and for dc electric field of the opposite sign. The dependences are shifted relative to each other, the phase difference is about 30°. In Fig. 3(b) the dependences of the SHG intensity vs electric field are shown for different anisotropy positions of the cell. The anisotropy position determines the contrast value of the ferroelectric switching dependences and the ratio between SHG responses corresponding to opposite biases. Ferroelectric switching, studied in reflection geometry and performed for the *pp* polarizations, also exhibits a shift of the anisotropy dependences for opposite electric fields with a phase difference of about 20°.

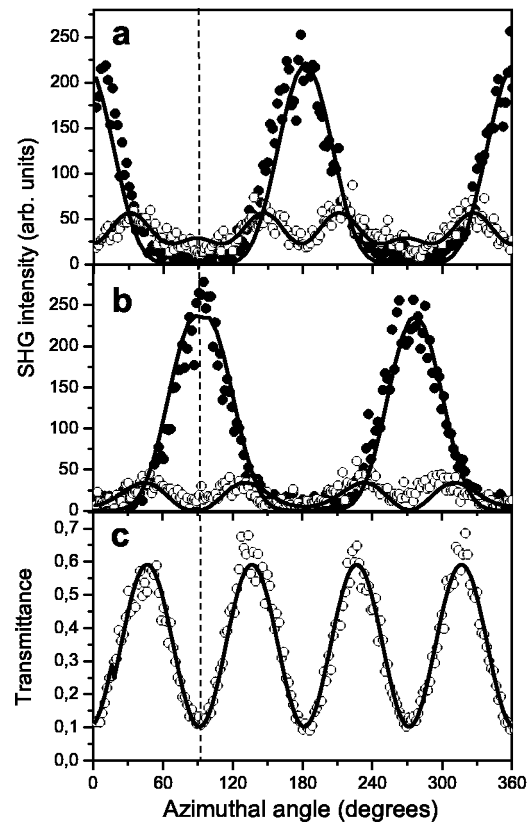


FIG. 2. Anisotropy dependence of the SHG intensity in transmission through the FLC cell in the Sm$C^*$ phase. (a) *ss* (filled circles) and *sp* (open circles) and (b) *pp* (filled circles) and *ps* (open circles) geometries. (c) Anisotropy dependence of the linear transmittance at cross-polarizers geometry in the Sm$C^*$ phase. Solid lines are calculated from theory.

The anisotropy of the linear-optical response in transmittance through the FLC cell is measured in crossed-polarizers geometry and is shown in Fig. 2(c). Application of the electric field leads to a shift of the linear transmittance anisotropy, as in the nonlinear case. In both cases, we observed a shift of about 30°.

Temperature dependences of the SHG response are taken in reflection geometry at the angle of incidence of about 45° and in transmission at normal incidence. The cases of the presence and absence of external dc field are studied. Figure 4(a) shows temperature dependences of the SHG intensity in *pp*-transmission geometry for biased (filled circles and squares) and unbiased (open circles) cells. In the absence of the electric field the temperature dependence of the SHG intensity approaches a constant value at critical temperature in accordance with a power law at $T<T_c$, and shows no manifestation of the surface EC effect at $T>T_c$ in the Sm$A^*$ phase. For biased LC samples, a critical behavior of the SHG intensity typical for the EC effect is obtained in the Sm$A^*$ phase in the vicinity of the phase transition.

## IV. DISCUSSION

FLC cell structure usually contains layers with different direction of spontaneous polarization—twisted or helicoidally wounded layers. This modulation of the space orientation of molecular dipoles is governed by the intermolecular

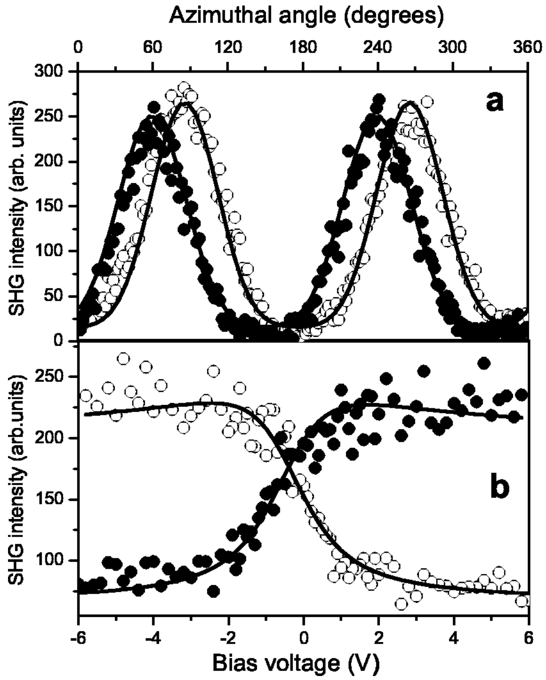


FIG. 3. (a) Anisotropy dependence of the SHG intensity in transmission geometry at different bias voltages applied: +8 V (filled circles), −8 V (open circles). Solid lines are calculated by Eq. (12); (b) SHG intensity dependence on the bias voltage in transmission for anisotropy positions 100 (open circles) and 230 (filled circles). Solid lines are calculated by Eqs. (12) and (13).

forces and substrate influence. We suppose that in the absence of the dc electric field the cell has a net dipole moment and the $C_2$ symmetry axis lying in the cell plane. Then it is possible to approximate the anisotropy dependences of SHG intensity in all the possible combinations of input and output polarizations in transmission at normal incidence by formulas analogous to Eq. (4) for *pp* case. In Fig. 2 the calculated curves are shown for all geometries. The approximation gives the ratios between in-plane components of nonlinear susceptibility

$$\chi_{xxy}:\chi_{yyy}:\chi_{yxx}=1:24:-3.3. \tag{5}$$

The linear transmittance anisotropy has four equal peaks and no dark extinction, which is typical for twisted structures. Assuming the main optical axis to lie in the cell plane, the approximation of the linear anisotropy dependence by Eq. (1) gives a birefringence of ∼0.083, which corresponds to the characteristic values for smectic LC measured by other authors [8]. The comparison of nonlinear and linear anisotropy dependences indicates that the $C_2$ symmetry axis, corresponding to the maximum of the SHG anisotropy in *pp* geometry, and the main optical axis, corresponding to the minimum of the linear transmittance anisotropy in *sp* geometry, are parallel.

Temperature dependences of the SHG intensity for the applied electric field of different polarities reveal a hysteresis-free Sm$C^*$–Sm$A^*$ second-order phase transition. A typical critical behavior in the vicinity of the Sm$C^*$–Sm$A^*$ phase transition is obtained. A nonzero SHG

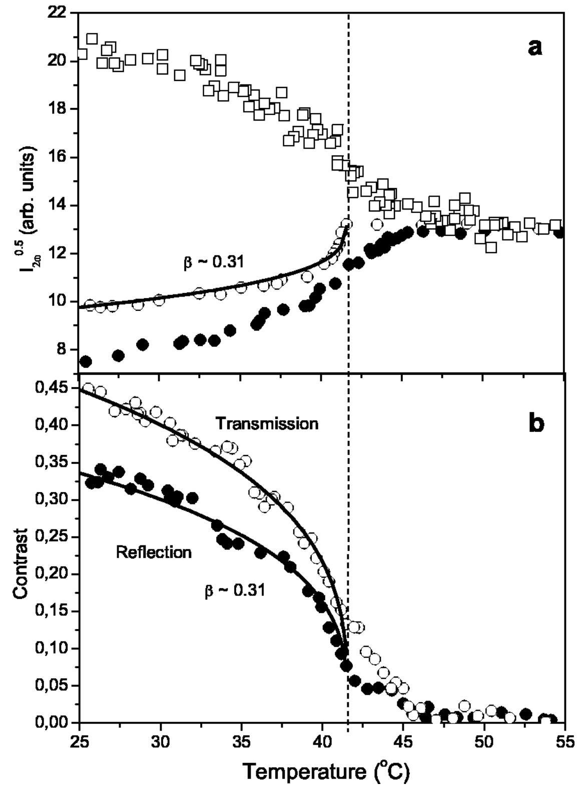


FIG. 4. (a) Temperature dependence of the SHG intensity in transmission geometry at different bias voltage applied: +8 V (squares), 0 V (open circles), −8 V (filled circles). Solid line is a fit by Eq. (8); (b) temperature dependence of the contrast in reflection (filled circles) and transmission (open circles) geometries. Solid lines are calculated by Eq. (11).

signal in the Sm$A^*$ phase denotes that some part of the cell is still oriented and has a polar order with an in-plane component of the nonlinear polarization. The temperature dependence of the SHG response for reflection geometry shows qualitatively the same behavior as in transmission geometry, which is connected with the Sm$C^*$–Sm$A^*$ phase transition in the subsurface layer of the cell. The SHG temperature dependence can be explained by the interference of the field- and temperature-dependent and field- and temperature-independent contributions to nonlinear polarization, responsible for the SHG signal. Then, we can write for the nonlinear polarization

$$\vec{P}^{2\omega}_{NL}=\vec{P}^{2\omega}_{surf}(E,T)+\vec{P}^{2\omega}_{bulk}(E,T)+\vec{P}^{2\omega}_{const}, \tag{6}$$

where $\vec{P}^{2\omega}_{surf}(E,T)$ and $\vec{P}^{2\omega}_{bulk}(E,T)$ are electric-field- ($E$) and temperature- ($T$) dependent contributions to the nonlinear polarization at double frequency from the subsurface layers and the bulk, respectively, and $\vec{P}^{2\omega}_{const}$ is a field- and temperature-independent component. For the transmitted SHG the correlation length is about 5 $\mu$m, while for reflection it is about 0.1 $\mu$m [14], which indicates that in reflection a thin subsurface layer participates in SHG. As SHG temperature dependences of subsurface layers and the bulk have the same qualitative character, then either $\vec{P}^{2\omega}_{bulk}(E,T)$ and $\vec{P}^{2\omega}_{surf}(E,T)$

from Eq. (6) should be the same functions of $E$ and $T$ or the bulk contribution to nonlinear polarization should vanish.

Explanation of temperature dependences demands the existence of an electric-field- and temperature-independent in-plane contribution $\vec{P}^{2\omega}_{const}$ to the nonlinear polarization. Orientation of the molecules in the bulk layers of the cell can be electric-field independent in some experimental geometries depending on the layer packing, but temperature dependence is obligatory because of the presence of the Sm$C^*$–Sm$A^*$ phase transition. Then the nonswitching layer should be in the subsurface region. We can assume that a ''frozen'' subsurface layer, with a thickness smaller than the correlation length for SHG in reflection geometry, exists. It is strongly stabilized by the surface coupling, and does not respond to any external electric-field or temperature variations, as well as the layer closest to the substrate. The latter has only $z$ component of the nonlinear polarization, as the dipole moments of its molecules are directed along the normal to the substrate plane, and then it does not contribute to the SHG at normal incidence. The in-plane spontaneous polarization can exist when the molecules rotate from layer to layer while moving from the surface to the bulk of the cell. Then the twist of the directors appears, resulting in the so-called twisted structure of the subsurface layers.

Let us figure out the interconnection between the temperature dependences of SHG and the order parameter of the Sm$C^*$–Sm$A^*$ phase transition. Usually the order parameter of this phase transition is the tilt angle, as spontaneous polarization is compensated because of the helical structure. The thickness of the cells studied in this paper is smaller than the helix pitch, besides, anisotropic interaction with the substrate produces an additional orientational order of the FLC molecules, so that the cells have spontaneous polarization $\vec{P}_{sp}$ in Sm$C^*$ phase. $\vec{P}_{sp}$ decreases in Sm$A^*$ phase and is a linear function of the tilt angle $\theta(E,T)$. So we can write for the SHG intensity

$$\sqrt{I^{2\omega}} \sim \vec{P}^{2\omega}_{NL} \sim \vec{P}_{sp} \sim \theta(E,T), \tag{7}$$

assuming that $\sqrt{I^{2\omega}(E,T)}$ has the same critical dependence on temperature as the tilt angle. Then, according to Eqs. (6) and (7), the temperature-dependent contribution $\sqrt{I^{2\omega}(E,T)}$ in the absence of the electric field and for $T<T_c$ can be approximated by the following expression:

$$\sqrt{I^{2\omega}(E=0)} \sim P^{2\omega}_{const} - P^{2\omega}_0 \left(1-\frac{T}{T_c}\right)^{\beta}, \tag{8}$$

where $P^{2\omega}_{const}$ and $P^{2\omega}_0$ are proportional to isotropic and anisotropic contributions of nonlinear polarizations, $T_c$ is the temperature of the phase transition, and $\beta$ is the critical exponent. Approximation of the curve is shown in Fig. 4(a) by a solid line, with $\beta=0.31$.

To compare the temperature behavior of the nonlinear polarization in the vicinity of the phase transition for reflection and transmission cases, we introduce the contrast of the dependences as

$$K = \frac{\sqrt{I^{2\omega}(+E)} - \sqrt{I^{2\omega}(-E)}}{\sqrt{I^{2\omega}(+E)} + \sqrt{I^{2\omega}(-E)}}, \tag{9}$$

where $I^{2\omega}(\pm E)$ are the SHG intensities for positive and negative voltages applied to the cell. In Fig. 4(b) the contrast vs temperature is shown for reflection and transmission geometries. The contrast determined in such a way shows a behavior similar to that of the order parameter near the phase transition. Introducing SHG intensity dependences on temperature in the presence of the electric field at $T<T_c$ in the way, analogous to Eq. (8),

$$\sqrt{I^{2\omega}(\pm E)} \sim P^{2\omega}_{const} \pm P^{2\omega}_0(\pm E)\left(1-\frac{T}{T_c}\right)^{\beta}, \tag{10}$$

and supposing $P^{2\omega}_0(E)=P^{2\omega}_0(-E)$, we can express the contrast $K$ as

$$K \sim \frac{P^{2\omega}_0(E)}{P^{2\omega}_{const}}\left(1-\frac{T}{T_c}\right)^{\beta}. \tag{11}$$

Approximation of the experimental dependences by Eq. (11) in Sm$C^*$ phase gives $\beta=0.31$ [Fig. 4(b)], as in the case of the absence of the dc electric field. The amplitude of the contrast (11) depends on the ratio $P^{2\omega}_0(E)/P^{2\omega}_{const}$ of field-dependent and -independent contributions to the nonlinear polarization. In transmission this ratio can be bigger due to the larger amount of layers participating in ferroelectric switching, besides, the field-independent contribution of the boundary layer leads to the contrast decrease in reflection geometry. These considerations explain why the contrast of the temperature dependences and electric-field-induced shift of the anisotropy dependences in transmission are bigger than in reflection geometry, as obtained in the experiment.

Temperature dependence of the contrast in the region of the EC effect, at $T>T_c$, exhibits a nonzero electric-field-dependent polarization vanishing at $\sim 10\,^{\circ}\mathrm{C}$ above the transition temperature. This indicates the presence of external dc-field-induced EC effect, taking place in the layers with electric-field- and temperature-dependent polarization.

Application of dc electric field to the FLC leads to a shift of the anisotropy dependences of the linear and nonlinear responses, as shown in Fig. 3(a). Similar pictures are obtained for the reflection geometry. As the character of anisotropy dependences is the same in the presence of the field, our suggestion of the switching mechanism based on the symmetry axis rotation in the cell plane seems to be rather realistic. The shift originates from the rotation of the molecules in the switching layers, the resulting nonlinear polarization of the cell is the sum of unchanged quadratic polarization from the frozen layer, and from field-dependent region with the new position of the symmetry axes. Thus for approximating the SHG anisotropy dependence in the presence of the electric field, we divide the nonlinear polarization into two parts, and Eq. (4) can be rewritten as

$$I^{2\omega}_{pp} \sim [g P^{2\omega}_{NL,pp}(\theta+d\theta) + (1-g) P^{2\omega}_{NL,pp}(\theta)]^2, \tag{12}$$

where $g$ is the effective thickness of the switching layer relative to the nonswitching one and $d\theta$ is a field-induced change of the azimuthal angle. The value of $g$ is estimated to be 0.5 which indicates that the magnitude of the field-independent contribution is comparable to the field-dependent one, allowing effective mutual interference in accordance with Eq. (6). Symmetry axis shift $d\theta$ between opposite values of the voltage is about 52°. For electric-field dependences of the SHG intensity, shown in Fig. 3(b), the independent variable is the electric field, and in Eq. (12) the azimuthal angle $\theta$ is fixed by the anisotropy position. Then $d\theta$ becomes a function of the electric field, chosen, according to Eq. (3), as a saturation function:

$$d\theta(E) = b \arctan[c(E - dE)], \tag{13}$$

where $b$ and $c$ are constants, depending on the strength of interaction between field and angle, and $dE$ is a constant determined by the history of ferroelectric switching, as it exhibits characteristic dc field hysteresis. Experimental dependences in Fig. 3(b) are taken for two anisotropy positions with the difference in $\theta \sim 130$ deg. Fitting one of the curves by Eq. (12) with Eq. (13) allows one to extract $b = 0.5$ and $c = 0.63$. Varying then only $dE$ and $\theta$ during approximation of the second curve gives the difference of the anisotropy position of about 126 deg, in good agreement with experimental conditions. Values of $dE$ in both cases lie in the region of typical hysteresis width and do not exceed 1 V/$\mu$m. The value of $b$ corresponds to the tilt of the symmetry axis in the cell plane, discussed above, Eq. (3).

In conclusion, the electroclinic effect, the Sm$C^*$–Sm$A^*$ phase transition and ferroelectric switching have been studied in thin planar cells of ferroelectric chiral liquid crystals by means of electro-optic and second harmonic generation techniques. The analysis of the temperature dependences of nonlinear quadratic response in the critical region leads to the assumption of a strong surface coupling existence, resulting in the stabilization of several frozen subsurface layers with the in-plane spontaneous polarization which is independent of the electric field and the temperature. The critical exponent is estimated to be $\sim 0.3$ in Sm$C^*$ phase in the vicinity of the Sm$C^*$–Sm$A^*$ phase transition. Ferroelectric switching has been observed while studying linear and nonlinear anisotropic responses and has been explained within a model, assuming an in-plane rotation of the symmetry and main optical axes of the cells in the presence of dc external electric field.

## ACKNOWLEDGMENTS

We thank Professor G. Heppke's group for synthesis of the samples used in our work. The work was supported by INTAS Grant No. 2002-113/F1b, President grant ''Leading Russian Scientific Schools'' Grant No. 1604.2003.2, and EU network Grant No. ERB FMRXCT 980209 (SILC). S.S. acknowledges funding from the European Regional Development Fund and from the Ministerio de Ciencia y Tecnologia through the Ramon y Cajal program.

[1] R.B. Meyer, L. Liebert, L. Strzelecki, and P. Keller, J. Phys. (Paris) **36**, L69 (1975).
[2] R.B. Meyer, Mol. Cryst. Liq. Cryst. **40**, 33 (1977).
[3] I. Musevic, R. Blinc, and B. Zeks, *The Physics of Ferroelectric and Antiferroelectric Liquid Crystals* (World Scientific, Singapore, 2000).
[4] P.G. de Gennes and J. Prost, *The Physics of Liquid Crystals* (Oxford University Press, New York, 1993); E. Olbrich, O. Marinov, and D. Davidov, Phys. Rev. E **48**, 2713 (1993).
[5] S. Garoff and R.B. Meyer, Phys. Rev. Lett. **38**, 848 (1977); Phys. Rev. A **19**, 338 (1979).
[6] W. Chen, Y. Ouchi, T. Moses, Y.R. Shen, and K.H. Yang, Phys. Rev. Lett. **68**, 1547 (1992); J. Xue and N.A. Clark, *ibid.* **64**, 307 (1990).
[7] J.V. Selinger, P.J. Collings, and R. Shashidhar, Phys. Rev. E **64**, 061705 (2002).
[8] M. Loddoch, G. Marowsky, H. Schmid, and G. Heppke, Appl. Phys. B: Lasers Opt. **59**, 591 (1994); B. Park, S. Seomun, M. Nakata, M. Takanashi, Y. Takanishi, K. Ishikawa, and H. Takezoe, Jpn. J. Appl. Phys., Part 1 **38**, 1474 (1999); N. Pereda, J. Ortega, C.L. Folcia, and J. Etxebarria, Phys. Rev. E **62**, 2334 (2000).
[9] N. Blombergen, R.K. Chang, S.S. Jha, and C.H. Lee, Phys. Rev. **174**, 813 (1968).
[10] Yariv and P. Yeh, *Optical Waves in Crystals* (Wiley, New York, 1983).
[11] Y. R. Shen, *The Principles of Nonlinear Optics* (Wiley, New York, 1984).
[12] B. Park, M. Nakata, S. Seomun, Y. Takanishi, K. Ishikawa, and H. Takezoe, Phys. Rev. E **59**, R3815 (1999).
[13] Yu.G. Fokin, T.V. Murzina, O.A. Aktsipetrov, S. Soria, and G. Marowsky, Surf. Sci. **507**, 724 (2002).
[14] Y.G. Fokin, T.V. Murzina, O.A. Aktsipetrov, S. Soria, and G. Marowsky, Appl. Phys. B: Lasers Opt. **74**, 777 (2002).